Open Journal of Applied Sciences, 2023, 13, 591-603
https://www.scirp.org/journal/ojapps
ISSN Online: 2165-3925
ISSN Print: 2165-3917

Simulation of Natural Convection Flow with Magneto-Hydrodynamics in a Wavy Top Enclosure with a Semi-Circular Heater

Mohammad Mahfuzul Islam[1], Md. Abdul Alim[2], Md. Mahmud Alam[1], Md. Jahirul Haque Munshi[3]

[1]Department of Mathematics, Dhaka University of Engineering and Technology (DUET), Gazipur, Bangladesh
[2]Department of Mathematics, Bangladesh University of Engineering and Technology (BUET), Dhaka, Bangladesh
[3]Department of Mathematics, Hamdard University Bangladesh (HUB), Hamdard Nagar, Gazaria, Munshiganj, Bangladesh
Email: mahfuzabir@gmail.com, maalim@math.buet.ac.bd, alamdr.mahmud@duet.ac.bd, drmunshi@hamdarduniversity.edu.bd

How to cite this paper: Islam, M.M., Alim, A.M., Alam, M.M. and Munshi, J.H.M. (2023) Simulation of Natural Convection Flow with Magneto-Hydrodynamics in a Wavy Top Enclosure with a Semi-Circular Heater. *Open Journal of Applied Sciences*, **13**, 591-603.
https://doi.org/10.4236/ojapps.2023.134047

Received: March 20, 2023
Accepted: April 25, 2023
Published: April 28, 2023

Abstract

Natural convection flow in enclosure has different applications such as room ventilation, heat exchangers, the cooling system of a building etc. The Finite-Element method based on the Galerkin weighted residual approach is used to solve two-dimensional governing mass, momentum and energy-equations for natural convection flow in the presence of a magnetic field on a roof top with semi-circular heater. In the enclosure the horizontal lower wall was heated, the vertical two walls were adiabatic, inside the semi-circular heater, the wavy top wall cooled. The parameters Rayleigh number, Hartmann number and Prandtl number are considered. The effects of the Hartmann number and Rayleigh number on the streamlines, isotherms, velocity profiles and average Nusselt number are examined graphically. The local Nusselt number and the average Nusselt number of the heated portion of the enclosure with the semi-circular heater are presented in this paper. Finally, for the validation of the existing work, the current results are compared with published results and the auspicious agreement is achieved.

Keywords

Natural Convection, Magneto-Hydrodynamics (MHD), Finite Element Method (FEM), Wavy Enclosure, Semi-Circular Heater

1. Introduction

The fluid flow and heat transfer of natural convection in cavity inside a semi-circular block has been studied by many researchers in the field of engineering applications. Nowadays many researchers have been working in wavy top enclosure. Azizul *et al.* [1] analyzed in the heatline visualization of mixed convection inside double lid-driven cavity having heated wavy wall present. Mahjabin and Alim [2] discussed the effect of Hartmann number on free convective flow of MHD fluid in a square cavity with a heated cone of different orientation. Bhuiyan and Alim [3] investigated the free convection in a square cavity with magnetic field where the semi-circular heat source is seen. Taghikhani and Chavoski [4] have studied internal heating in a square cavity in MHD free convection. Oztop and Salem [5] discussed the effects of Joule heating on MHD natural convection in non-isothermally heated enclosure. They analyzed that the stream function decreased with the increasing of Hartmann number. Chamkha [6] studied the hydromagnetic combined convection flow in a vertical lid-driven cavity with internal heat generation. A comprehensive reviewed the problem that involved mixed convection in different shapes of enclosures such as triangular, rectangular, square, trapezoidal etc discussed by Molana *et al.* [7]. Parvin and Nasrin [8] analyzed the flow and heat transfer for MHD free convection in an enclosure. Besides Koseff *et al.* [9] studied the process of mixed convection enclosed by re-circulating flow cross section in the insulated lid-driven rectangular cavity. In addition, mixed convection in a complex shape of geometry in a triangular cavity with moving walls had been analyzed by Rabani [10]. Basak *et al.* [11] discussed heat lines based natural convection analysis in tilted isosceles triangular enclosures with linearly heated inclined walls for the effect of various orientations. Rudraiah *et al.* [12] studied the effect of magnetic field on free convection in a rectangular enclosure. Hossain *et al.* [13] discussed a finite element analysis on MHD free convection flow in open square cavity containing heated circular cylinder. Jani *et al.* [14] studied the magneto-hydrodynamic free convection in a square cavity heated from below and cooled from other walls. To the best of authors' knowledge none of the above mentioned studies have addressed the present problem. Hence the present work provides the fluid flow and heat transfer in a wavy top enclosure in presence of semi-circular heater and magnetic field. The numerical results are presented graphically in terms of stream lines, isothermal lines and average Nusselt number and then discussed.

2. Diagram and Calculation Framework

The physical diagram of the system is shown in **Figure 1**. Thermo-physical properties of the fluid in the flow are assumed. Consider the laminar convection flow in the enclosure of height H and width L filled with an electrically conducting fluid which generates the heat determined by the temperature difference between the fluid and the wall. The upper portion of the wavy enclosure is cold (T_c) the vertical wall is adiabatic. The lower portion and inside the semi-circular block are heated (T_h).

The above physical model, using the coordinate system shown in **Figure 1**, the governing equation can be written in the dimensional form.

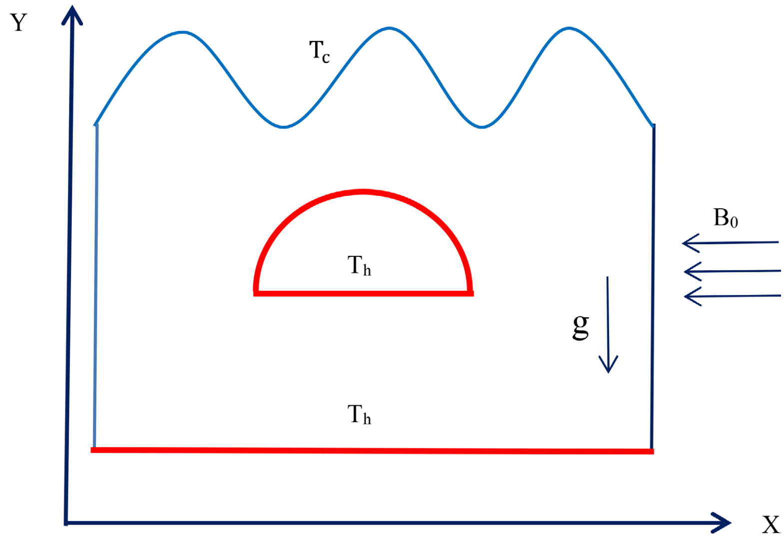

Figure 1. Physical model of convection in a wavy top enclosure.

$$\frac{\partial u}{\partial x}+\frac{\partial v}{\partial y}=0 \tag{1}$$

$$u\frac{\partial u}{\partial x}+v\frac{\partial u}{\partial y}=-\frac{1}{\rho}\frac{\partial p}{\partial x}+\nu\left(\frac{\partial^2 u}{\partial x^2}+\frac{\partial^2 u}{\partial y^2}\right) \tag{2}$$

$$u\frac{\partial v}{\partial x}+v\frac{\partial v}{\partial y}=-\frac{1}{\rho}\frac{\partial p}{\partial y}+\nu\left(\frac{\partial^2 v}{\partial x^2}+\frac{\partial^2 v}{\partial y^2}\right)+g\beta\left(T-T_c\right)-\frac{\sigma B_0^2 v}{\rho} \tag{3}$$

$$u\frac{\partial T}{\partial x}+v\frac{\partial T}{\partial y}=\alpha\left(\frac{\partial^2 T}{\partial x^2}+\frac{\partial^2 T}{\partial y^2}\right) \tag{4}$$

Dimensional Boundary Condition:

Walls	Boundary conditions
Top wavy wall	$u=v=0, T=T_c, 0\le x\le L,\ \ y=\frac{L}{2}\left(1+\sin 2n\pi x\right)$
Bottom wall	$u=v=0, T=T_h, 0\le x\le L$
Left wall	$u=0, v=0, \frac{\partial T}{\partial x}=0, 0\le y\le \frac{L}{2}$
Right wall	$u=0, v=0, \frac{\partial T}{\partial x}=0, 0\le y\le \frac{L}{2}$

Now, using the following dimensionless variables:

$$X=\frac{x}{L}, Y=\frac{y}{L}, U=\frac{uL}{\alpha}, V=\frac{vL}{\alpha}, P=\frac{pL^2}{\rho\alpha^2}, \theta=\frac{T-T_c}{T_h-T_c},$$

$$Pr=\frac{\nu}{\alpha}, Gr=\frac{g\beta\left(T_h-T_c\right)L^3}{\nu^2}, Ra=Pr\cdot Gr,$$

$$Ha^2=\frac{\sigma B_0^2 L^2}{\mu}, \sigma=\frac{\rho^2\alpha}{L^2}, \alpha=\frac{\kappa}{\rho C_p}$$

Then the dimensionless equations are,

$$\frac{\partial U}{\partial X}+\frac{\partial V}{\partial Y}=0 \tag{5}$$

$$U\frac{\partial U}{\partial X}+V\frac{\partial U}{\partial Y}=-\frac{\partial P}{\partial X}+Pr\left[\frac{\partial^2 U}{\partial X^2}+\frac{\partial^2 U}{\partial Y^2}\right] \tag{6}$$

$$U\frac{\partial V}{\partial X}+V\frac{\partial V}{\partial Y}=-\frac{\partial P}{\partial Y}+Pr\left[\frac{\partial^2 V}{\partial X^2}+\frac{\partial^2 V}{\partial Y^2}\right]+RaPr\theta-Ha^2PrV \tag{7}$$

$$U\frac{\partial \theta}{\partial X}+V\frac{\partial \theta}{\partial Y}=\left[\frac{\partial^2 \theta}{\partial X^2}+\frac{\partial^2 \theta}{\partial Y^2}\right] \tag{8}$$

Dimensionless Boundary Conditions:

Walls	Boundary conditions
Top wavy wall	$U=V=0,\theta=0$
Bottom wall	$U=V=0,\theta=1$
Left wall	$U=0,V=0,\frac{\partial\theta}{\partial N}=0$
Right wall	$U=0,V=0,\frac{\partial\theta}{\partial N}=0$

The heat transfer coefficient in terms of local Nusselt number (*Nu*) is defined by,

$$Nu=-\frac{\partial\theta}{\partial\eta}$$

Where η is the outward drawn normal on the plane.

Dimensionless normal temperature gradient can be,

$$\frac{\partial\theta}{\partial\eta}=\sqrt{\left(\frac{\partial\theta}{\partial X}\right)^2+\left(\frac{\partial\theta}{\partial Y}\right)^2}$$

While the average Nusselt number $\overline{Nu}$ is obtained by integrating the local Nusselt number along the bottom surface of wavy enclosure and is defined by

$$\overline{Nu}=-\frac{1}{L}\int_0^L\frac{\partial\theta}{\partial\eta}\mathrm{d}s$$

where S is the dimensionless coordinate along the circular surface.

If $L = 1$ for length of the enclosure then,

$$\overline{Nu}=-\int_0^1\frac{\partial\theta}{\partial\eta}\mathrm{d}s$$

3. Numerical Technique

The dimensional governing equations of my physical problem are converted into the dimensionless form. The governing equations along with the boundary conditions are solved numerically, employing Finite Element Method [15] based on Galerkin-Weighted Residual formulation. To ensure convergence of solutions the following criteria is applied to all dependent variables over the solution domain,

$$\sum \left| \phi_{i,j}^{n} - \phi_{i,j}^{n-1} \right| \le 10^{-5}$$

where ϕ represents the dependent variables *U, V, P* and *T* the indexes *i,j* refers to space coordinates and the index *n* is the current iteration.

4. Program Validation

Comparison between streamlines and isotherms for graphical solution are shown in **Figure 2**. It is clear from the figures that there is an excellent agreement between two results.

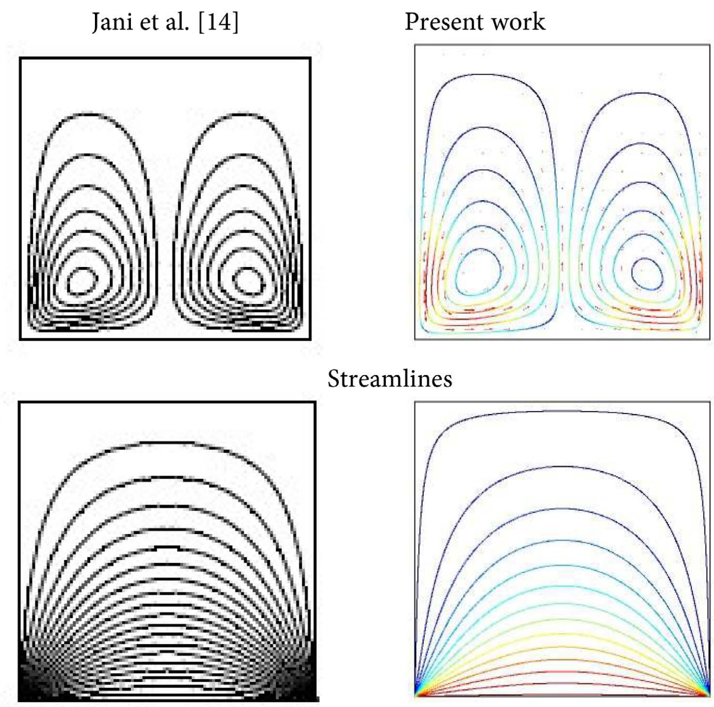

Figure 2. Comparison between streamlines and isotherms for graphical solution of (a) Jani *et al.* [14] and (b) Present Study at $Ra = 10^4$, $Ha = 50$.

5. Results and Discussion

In this section, results of the simulation of natural convection flow with Magneto-hydrodynamics in a wavy top enclosure with a semi-circular heater presented in numerical and graphical. The results have been obtained for the Hartmann number Ha = 10, 25, 50,100 and the Rayleigh number Ra = 100, 1000, 5000, 10,000. The results are illustrated with streamlines, isotherms, velocity profiles, local Nusselt number and average Nusselt number.

5.1. Effects of Hartmann Number

The effects of Hartmann number Ha = 10, 25, 50,100 where Ra = 1000, Pr = 0.71

analyzed by **Figure 3**. The fluid movement can be visualized from streamlines while the isothermal lines show the temperature distribution. For *Ha* = 10 while the circulation of fluid in the left and right side of the semi-circular block is significant and the fluid moves by two circulation cells. From isothermal lines we see that heat transfer from heated block and bottom wall to the cold portion of fluid.

The streamlines curve for *Ha* = 25, the top corner of the wavy cavity two vortices are visible. For the value of *Ha* increasing the flow circulation appears slow than the figure when *Ha* = 10. The isothermals curve for *Ha* = 25 the heat of surrounding block is lightly decrease than the when *Ha* = 10. Bottom side of the enclosure the heat increasing visualizes. For *Ha* = 50, the fluid circulation of streamlines gradually slow than the previous position and upper corner of the enclosure appear two vortices with increasing flow movement and the left and right side of block appears vortices also. For *Ha* = 50 the isothermals curve of the left and bottom corner of heat gradually increase and the heat of surrounding the block gradually slowdown.

For *Ha* = 100 the fluid flow gradually slowdown of streamlines and the vortices shape of the corner of upper side of the wavy cavity increases. Surrounding

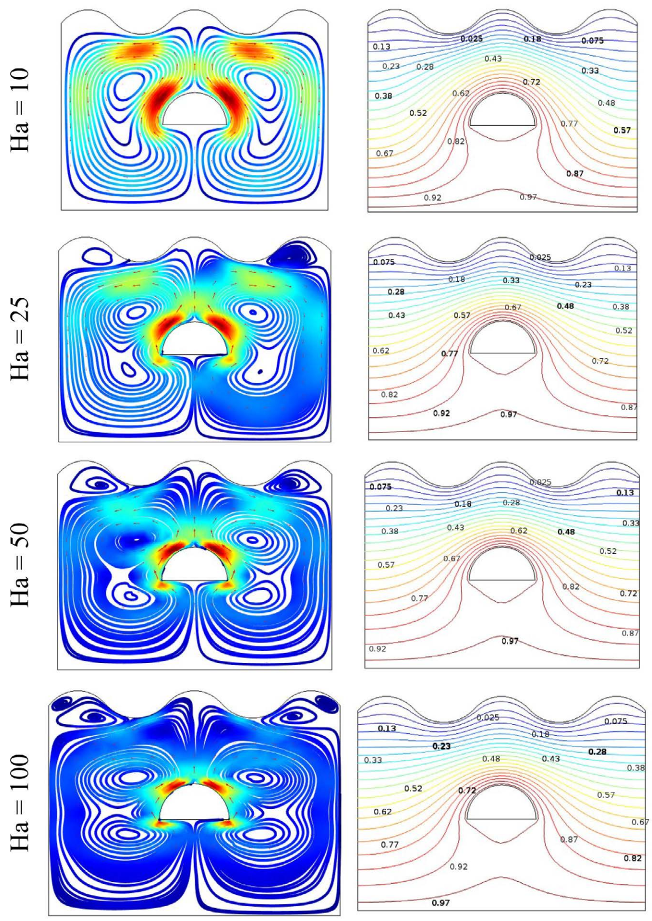

Figure 3. Streamlines and Isotherms for the different values of Hartmann number when *Ra* = 1000 and *Pr* = 0.71.

the semicircular block the vortices also increasing which appears the fluid flow slowdown. For *Ha* = 100 the heat of the isothermals curve gradually decreases surrounding the block. For increasing of Hartmann number the heat slowdown.

5.2. Variation of Rayleigh Number

Figure 4 shows the streamlines and isotherms for different values of Rayleigh number for *Pr* = 0.71 and *Ha* = 25. For *Ra* = 100 the streamlines of fluid is visualized and upper corner of the wavy enclosure created two vortices. The flow circulates both sides of the semicircular block in the enclosure. From the left side of block the flow towards right to left and the other right side the flow moves left to right. For *Ra* = 100 the isothermals curve indicates that heat generated from bottom to top in the enclosure. The streamlines of fluid for *Ra* = 1000 the fluid flow movement increasing than the stage of *Ra* = 100. Here the upper corner and internal of the enclosure vortices are visualized and the isothermals curve indicates that for *Ra* = 1000 the heat of enclosure increasing for the increasing of fluid movement than the stage of previous position and the upper side of block the heat increasing are seen.

For *Ra* = 5000 the streamlines of fluid movement increasing and the upper side of enclosure shows heated flow movement visualized also. The isothermals

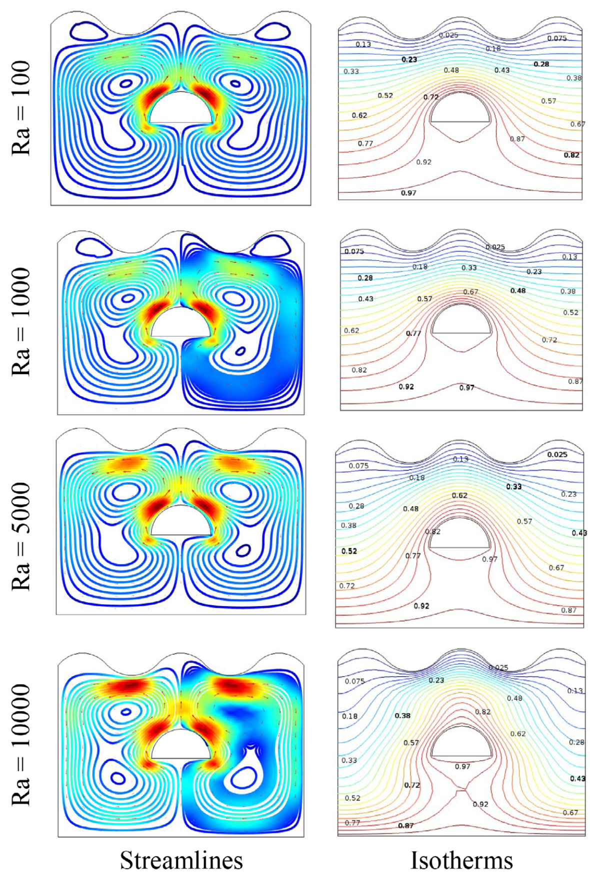

Figure 4. Streamlines and isotherms for the different values of Rayleigh numbers when *Ha* = 25 and *Pr* = 0.71.

for *Ra* = 5000 the heated flow increasing from bottom to top and the upper side of semi-circular block. The heated flow curve pattern increasing. The streamlines of fluid for *Ra* = 10,000 are visualized than the previous stage and the heated flow is more increasing. The isothermals curve indicates that for *Ra* = 10,000 heat increasing from bottom to top of the wavy enclosure is more than the stage of *Ra* = 5000.

5.3. Velocity Profile of Different Hartmann Number and Rayleigh Number

Figure 5 shows that the magnetic field effect of fluid when Hartmann number increases for *Ha* = 10, 25, 50, 100 the velocity profile gradually decreases while *Pr* = 0.71 and *Ra* = 1000. The y-component of fluid velocity in the enclosure is about to become horizontal as the magnetic field strength gradually increase.

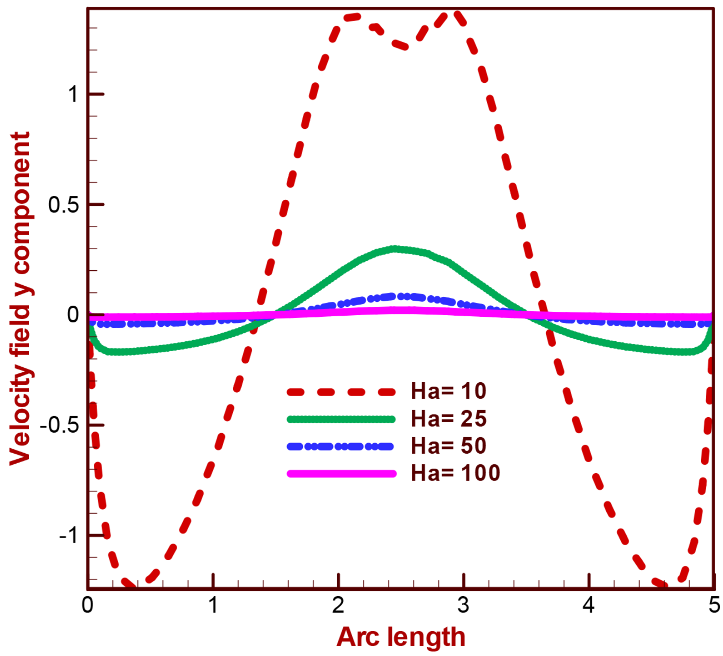

Figure 5. Effect of velocity profiles along y-component of the enclosure with different values of Hartmann number *Ha* = 10, 25, 50, 100 when *Ra* = 1000 and *Pr* = 0.71.

Again Figure 6 shows that the magnetic field effect of fluid when Rayleigh number increases for *Ra* = 100, 1000, 5000, 10,000 the velocity profile gradually increases while *Pr* = 0.71 and *Ra* = 1000. The velocity of y-component of fluid flow for low Rayleigh number in the enclosure is become horizontal. For the high value of *Ra* the fluid flow is increasing of velocity.

Again the effect of velocity profiles along y-component of the enclosure with different values of Rayleigh number *Ra* = 100, 1000, 5000, 10,000 when *Ha* = 25 and *Pr* = 0.71 are shown in Figure 6. As seen from this figure maximum and minimum velocity profiles are here. For lower value of Rayleigh number velocity profiles are less significant change and parallel to horizontal line. Also, for higher value of Rayleigh number velocity profiles are more significant change.

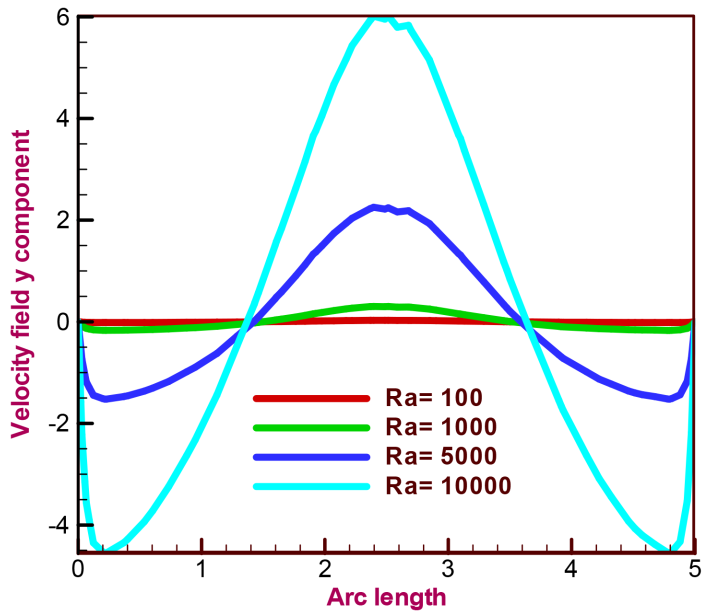

Figure 6. Effect of velocity profiles along y-component of the enclosure with different values of Rayleigh number Ra = 100, 1000, 5000, 10,000 when Ha = 25 and Pr = 0.71.

5.4. Variation of Local Nusselt Number and Dimensionless Temperature

The variation of local Nusselt number along are Y-axis of the wavy enclosure with different values of Hartmann numbers with Ha = 10, 25, 50, 100 when Ra = 100, Pr = 0.71 are shown in Figure 7. As seen from this figure minimum and maximum shape curves obtained here. The lower value of Hartmann number local Nusselt number is more significant change but higher value of Hartmann number is less significant number.

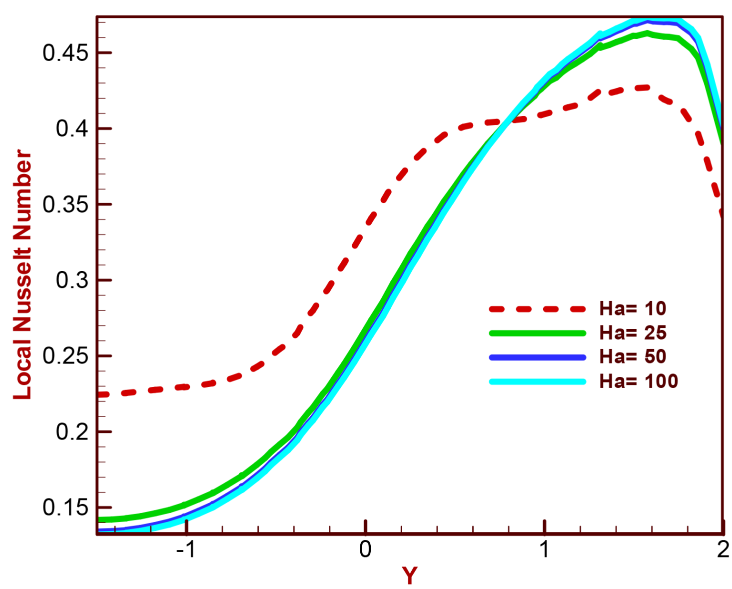

Figure 7. Variation of local Nusselt number along Y-axis at X = 1 of the enclosure with different values of Hartmann numbers Ha = 10, 25, 50, 100 when Ra = 100, Pr = 0.71.

Figure 8 presents the variation of dimensionless temperature along the *Y*-axis for different Hartmann numbers with Ha = 10, 25, 50, 100 when Ra = 100, Pr = 0.71. As seen from the figure, temperature value is increased from the increasing of Hartmann number.

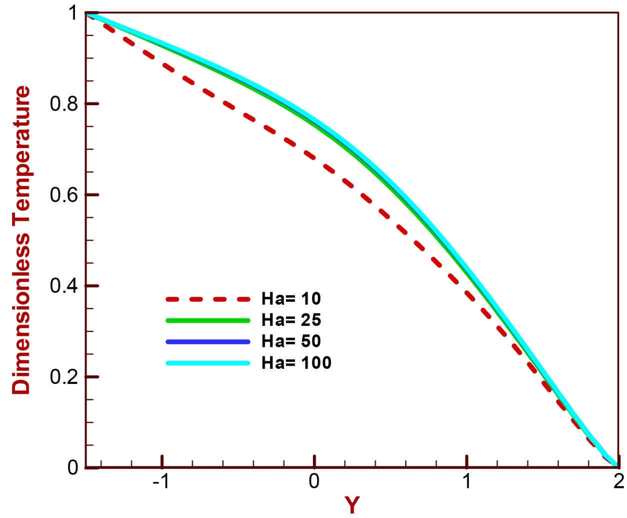

Figure 8. Variation of dimensionless temperature along *Y*-axis at $X = 1$ of the enclosure with different values of Hartmann numbers Ha = 10, 25, 50, 100 when Ra = 100, Pr = 0.71.

5.5. Average Nusselt Number versus of Ha and Ra

In this section, simulation of natural convection flow with Magneto-hydrodynamics in a wavy top enclosure with a semi-circular heater is numerically presented. The average Nusselt number versus Rayleigh numbers with different values Prandtl number are shown in Figure 9. It can be seen from this figure, the average

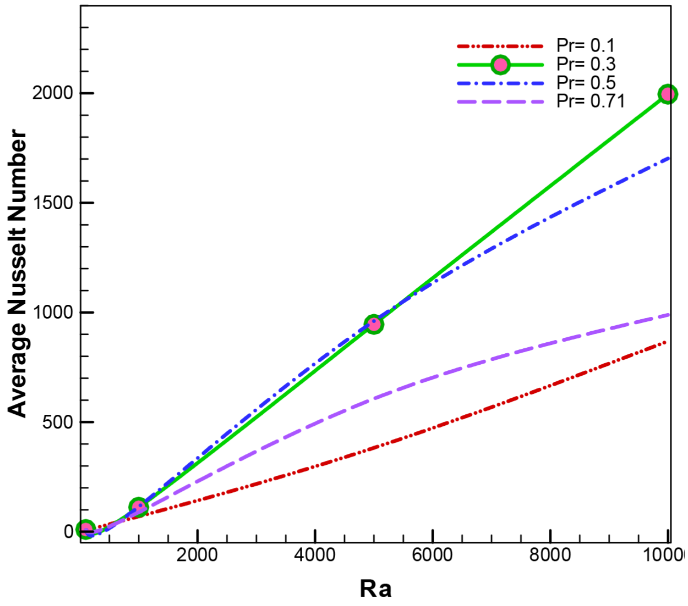

Figure 9. Variation of average Nusselt number versus Rayleigh numbers for different values of Prandtl numbers with Ha = 50.

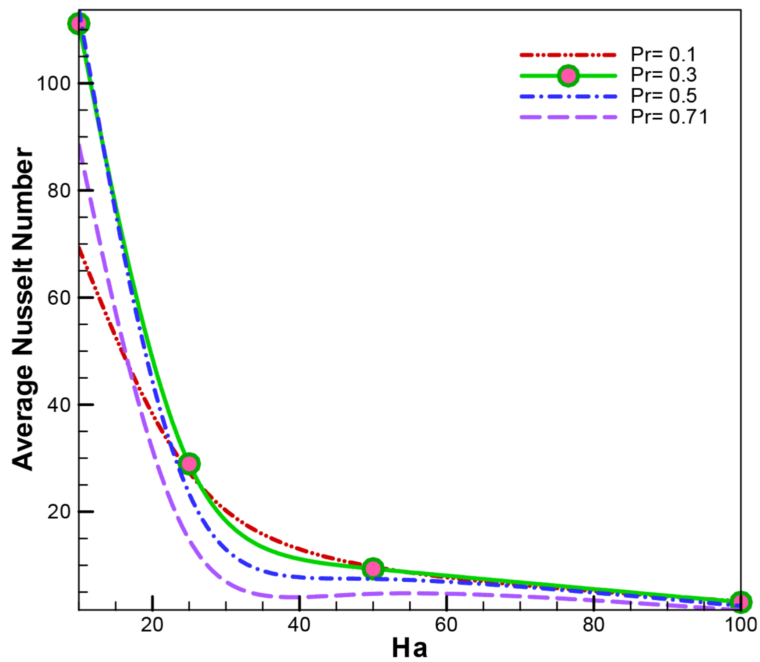

Figure 10. Variation of average Nusselt number versus Hartmann numbers for different values of Prandtl numbers with $Ra = 1000$.

Nusselt number increases when the value of the Prandtl number increases.

Also, the average Nusselt number versus Hartmann numbers with different values Prandtl number are shown in **Figure 10**. The minimum average Nusselt number is obtained for the lowest Prandtl number.

6. Conclusion

The convection flow discussed here is in which the bottom wall and inside block are heated in a wavy top enclosure. The present investigation observed the streamlines and isotherms in presence of MHD in the enclosure. Firstly, it is clear that with the increase in the Hartmann number (*Ha*) of the fluid flow, the velocity profile decreases in the enclosure. Again we observed that with the increment of *Ha*, the temperature profile gradually decreases. For the increasing values of Rayleigh number (Ra) the flow velocity in the enclosure gradually increases. Finally, the average Nusselt number of fluid flow decreases as the values of Hartmann number (Ha) increases. Also the average Nusselt number of the fluid flow gradually increases for the higher values of Rayleigh number (Ra).

Conflicts of Interest

The authors declare no conflicts of interest regarding the publication of this paper.

References

[1] Azizul, F.M., Alsabry, A.I., Hashim, I. and Chamkha, A.J. (2020) Heatline Visualization of Mixed Convection inside Double Lid-Driven Cavity having Heated Wavy Wall. *Journal of Thermal Analysis and Calorimetry*, **145**, 3159-3176.

https://doi.org/10.1007/s10973-020-09806-5

[2] Mahjabin, S. and Alim, M.A. (2018) Effect of Hartmann Number on Free Convective Flow of MHD Fluid in a Square Cavity with a Heated Cone of Different Orientation. *American Journal of Computational Mathematics*, **8**, 314-325. https://doi.org/10.4236/ajcm.2018.84025

[3] Bhuiyan, A.H. and Alim, M.A. (2014) Study of Free Convection in a Square Cavity with Magnetic Field and Semi Circular Heat Source of Different Orientations. *Procedia Engineering*, **90**, 445-451. https://doi.org/10.1016/j.proeng.2014.11.754

[4] Taghikhani, M.A. and Chavoshi, H.R. (2013) Two Dimensional MHD Free Convection with Internal Heating in a Square Cavity. *Thermal Energy and Power Engineering*, **2**, 22-28.

[5] Oztop, F.H. and Al-Salem, K. (2012) Effects of Joule Heating on MHD Natural Convection in Non-Isothermally Heated Enclosure. *Journal of Thermal Science and Technology*, **32**, 81-90.

[6] Chamkha, A.J. (2002) Hydromagnetic Combined Convection Flow in a Vertical Lid-Driven Cavity with Internal Heat Generation or Absorption. *Numerical Heat Transfer*, *Part A*, **41**, 529-546. https://doi.org/10.1080/104077802753570356

[7] Izadi, S., Armaghani, T., Ghasemiasl, R., Chamkha, A.J. and Molana, M. (2019) A Comprehensive Review on Mixed Convection of Nanufluids in Various Shapes of Enclosure. *Powder Technology*, **343**, 880-907. https://doi.org/10.1016/j.powtec.2018.11.006

[8] Parvin, S. and Nasrin, R. (2011) Analysis of the Flow and Heat Transfer Characteristics for MHD Free Convection in an Enclosure with a Heated Obstacle. *Nonlinear Analysis*: *Modelling and Control*, **16**, 89-99. https://doi.org/10.15388/NA.16.1.14117

[9] Prasad, A.K. and Koseff, J.R. (1996) Combined Forced and Natural Convection Heat Transfer in a Deep Lid-Driven Cavity Flow. *International Journal of Heat and Fluid Flow*, **17**, 460-467. https://doi.org/10.1016/0142-727X(96)00054-9

[10] Rabani, M. (2019) Numerical Analysis of Mixed Convection Heat Transfer in a Triangular Cavity with Moving Walls. *Heat Transfer Research*, **50**, 463-485. https://doi.org/10.1615/HeatTransRes.2018025276

[11] Basak, T., Anandalakshmi, R. and Roy, M. (2013) Heatlines Based Natural Convection Analy sis in Tilted Isoceles Triangular Enclosures with Linearly Heated Inclined Walls: Effect of Various Orientations. *International Communications in Heat and Mass Transfer*, **43**, 39-45. https://doi.org/10.1016/j.icheatmasstransfer.2013.01.008

[12] Rudraiah, N., Baroon, R.M., Venkatachalappa, M. and Subbaraya, C.K. (1995) Effect of a Magnetic Field on Free Convection in a Rectangular Enclosure. *International Journal of Engineering and Science*, **33**, 1075-1084. https://doi.org/10.1016/0020-7225(94)00120-9

[13] Hossain, S.A., Alim, M.A. and Saha, S.K. (2015) A Finite Element Analysis on MHD Free Convection Flow in Open Square Cavity Containing Heated Circular Cylinder. *American Journal of Computational Mathematics*, **5**, 41-54. https://doi.org/10.4236/ajcm.2015.51003

[14] Jani, S., Mahmoodi, M. and Amini, M. (2013) Magnetohydrodynamic Free Convection in a Square Cavity Heated from Below and Cooled from Other Walls. *International Journal of Mechanical*, *Aerospace*, *Industrial*, *Mechatronic and Manufacturing Engineering*, **7**, 750-755.

[15] Reddy, J.N. (1993) An Introduction to Finite Element Method. McGraw-Hill, New York.

Nomenclature

B_0	Applied magnetic field
C_p	Fluid specific heat
g	Gravitational acceleration
H	Enclosure height
L	Enclosure width
Gr	Grashof number
k	Fluid thermal conductivity
$\overline{Nu}$	Average Nusselt number
p	Fluid pressure
P	Non-dimensional pressure of the fluid
Pr	Prandtl number
Ha	Hartmann number
Ra	Rayleigh number
T	Temperature
T_c	Cold temperature
T_h	Heated temperature
ΔT	Temperature difference
u, v	Dimensional velocity components
U, V	Dimensionless velocity component
x, y	Dimensional Cartesian coordinates
X, Y	Dimensionless Cartesian coordinates

Greek Symbols

α	Fluid thermal diffusivity
β	Coefficient of thermal expansion of fluid
μ	Fluid dynamic viscosity
ν	Fluid kinematic viscosity
σ	Fluid electrical conductivity
θ	Dimensionless temperature
ρ	Density of the fluid

Subscripts

c	cold
h	heated